Earth and Planetary Science Letters 431 (2015) 164–172

Contents lists available at ScienceDirect

Earth and Planetary Science Letters

www.elsevier.com/locate/epsl

Explosive volcanism in complex impact craters on Mercury and the Moon: Influence of tectonic regime on depth of magmatic intrusion

Rebecca J. Thomas [a,*], David A. Rothery [a], Susan J. Conway [a], Mahesh Anand [a,b]

[a] Department of Physical Sciences, The Open University, Walton Hall, Milton Keynes, MK7 6AA, UK
[b] Department of Earth Sciences, Natural History Museum, Cromwell Road, London, SW7 5BD, UK

ARTICLE INFO

Article history:
Received 6 February 2015
Received in revised form 24 August 2015
Accepted 6 September 2015
Available online 30 September 2015
Editor: C. Sotin

Keywords:
Mercury
Moon
explosive volcanism
impact crater
intrusion

ABSTRACT

Vents and deposits attributed to explosive volcanism occur within numerous impact craters on both the Moon and Mercury. Given the similarities between the two bodies it is probable that similar processes control this spatial association on both. However, the precise morphology and localization of the activity differs on the two bodies, indicating that the nature of structures beneath impact craters and/or volcanic activity may also be different. To explore this, we analyze sites of explosive volcanism within complex impact craters on the Moon and Mercury, comparing the scale and localization of volcanic activity and evidence for post-formation modification of the host crater. We show that the scale of vents and deposits is consistently greater on Mercury than on the Moon, indicating greater eruption energy, powered by a higher concentration of volatiles. Additionally, while the floors of lunar craters hosting explosive volcanism are commonly fractured, those on Mercury are not. The most probable explanation for these differences is that the state of regional compression acting on Mercury's crust through most of the planet's history results in deeper magma storage beneath craters on Mercury than on the Moon. The probable role of the regional stress regime in dictating the depth of intrusion on Mercury suggests that it may also play a role in the depth of sub-crater intrusion on the Moon and on other planetary bodies. Examples on the Moon (and also on Mars) commonly occur at locations where flexural extension may facilitate shallower intrusion than would be driven by the buoyancy of the magma alone.

1. Introduction

It has long been recognized that vents and deposits attributed to explosive volcanism frequently occur within complex impact craters on the Moon (e.g., Schultz, 1976; Head and Wilson, 1979; Coombs and Hawke, 1992). More recently, data from the MErcury Surface, Space ENvironment, GEochemistry, and Ranging (MESSENGER) spacecraft have revealed that an association between putative explosive volcanism and impact craters also exists on Mercury (Gillis-Davis et al., 2009; Thomas et al., 2014b). Mercury and the Moon are similar in several respects: they are virtually airless, and have a surface geology that is dominated by a combination of impact cratering and volcanic resurfacing. The similar localization of explosive volcanic activity on both bodies, therefore, suggests the action of similar processes.

In the lunar case, it has been proposed that localization of explosive volcanism within impact craters results from density-trapping of magma in the brecciated zone below the crater (Head and Wilson, 1979). In this model, a vertically-propagating dike encounters the low density, weak material of the breccia lens beneath the crater floor and is diverted to form a sill because the density and rigidity contrast favors lateral propagation rather than continued vertical ascent (Schultz, 1976; Wichman and Schultz, 1995a). With continued recharge, this sill propagates horizontally until it encounters higher lithostatic pressures at the wall zone (Thorey and Michaut, 2014) and the intrusion begins to thicken, fracturing the floor above. Dike propagation to the surface is commonly favored along zones of extension at the intrusion margins (Pollard and Johnson, 1973) and results in either effusive volcanism, forming lava pools, or, if sufficient exsolved gas builds up prior to eruption, explosive volcanism (Jozwiak et al., 2015). The products of both of these styles of volcanism are observed at circumferential fractures in floor-fractured craters (FFCs) on the Moon, so this appears to be a good explanatory model.

On Mercury, too, there is evidence for sub-crater magma storage prior to eruption. Endogenic pits surrounded by a spectrally-distinct deposit, interpreted as volcanic vents (Kerber et al., 2009), often occur in groups within a single crater, indicating a shared proximal source for coeval and/or sequential eruptions. Moreover, the scale and morphology of vents and deposits are consistent with

* Corresponding author. Tel.: +44 (0)1908 858535.
E-mail address: rebecca.thomas@open.ac.uk (R.J. Thomas).

http://dx.doi.org/10.1016/j.epsl.2015.09.029

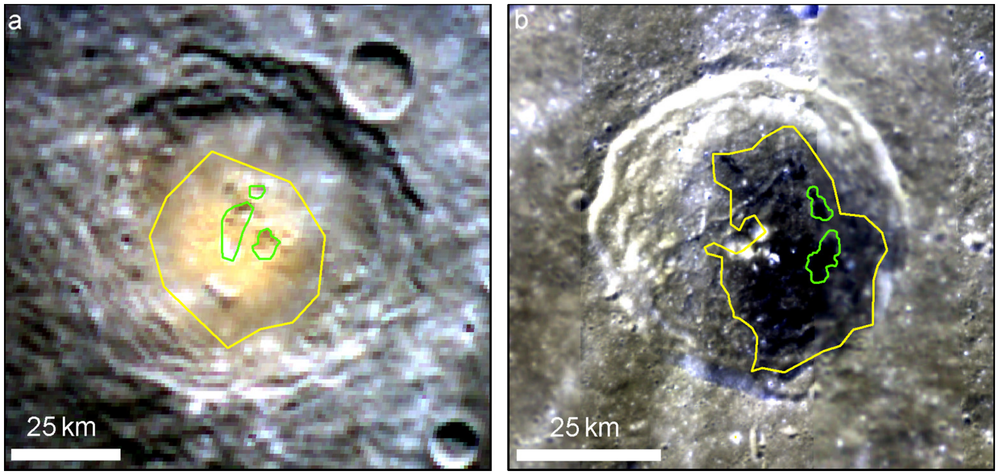

Fig. 1. Spectral anomalies with diffuse margins interpreted as pyroclastic deposits on (a) Mercury and (b) the Moon. Yellow outline: extent of the spectral anomaly, green outline: rim of candidate vent. (a) Rilke crater (pit group 8026). Color composite of MDIS WAC images EW0222970395I (996 nm), EW0222970415G (749 nm), and EW0222970399F (433 nm) (NASA/JPL-Caltech) in the red, green and blue bands. (b) Franklin crater. Excerpt from the Clementine UVVIS global mosaic with reflectance at 1000 nm, 900 nm, and 415 nm and in the red, green and blue bands. (For interpretation of the references to color in this figure, the reader is referred to the web version of this article.)

accumulation of volatiles in a subsurface magma chamber prior to eruption (Thomas et al., 2014b). The occurrence of the majority (79%) of explosive volcanic vents surrounded by putative pyroclastic deposits within impact craters on Mercury also supports the hypothesis that the subsurface structure of craters plays a controlling role in the localization of explosive volcanism. However, the specific character of this volcanism differs from that on the Moon. Floor-fracturing is observed in only one impact crater on Mercury (Head et al., 2009), and this does not host a pyroclastic vent or deposit. Additionally, explosive volcanism commonly occurs at and around central uplifts in craters on Mercury, rather than at the outer margin of the floor (Thomas et al., 2015).

The contrasting character of volcanism and host-crater modification between the Moon and Mercury indicates that it cannot be assumed that magma rise beneath impact craters on terrestrial bodies will always result in the eruptive character familiar from the Moon. An investigation into probable controls on crater-localized magma rise, storage, and explosive eruption on each body has the potential to enhance our understanding of tectono-magmatic conditions on both bodies. To this end, we have investigated the dimensions and settings of pits and deposits thought to result from explosive volcanism within complex impact craters on the Moon and Mercury. Using these data, we have characterized the energy of eruption and deformation of host craters and thereby placed constraints on the probable controls on intrusion and eruption. Our findings suggest that the regional stress regime played an important role in the depth of magma intrusion on Mercury, and may also have done so on the Moon.

2. Data and methods

2.1. Site selection

We analyzed 16 sites on Mercury and 15 on the Moon where an impact crater hosts candidate volcanic vents surrounded by a diffuse-margined spectral anomaly generally accepted to indicate a pyroclastic deposit (Table S1). Only sites occurring within complex impact craters were selected (30–120 km diameter on Mercury Pike, 1988, and 30–140 km on the Moon, Pike, 1980), so that subsurface crater-related structures could be considered broadly comparable across the sample set.

On both bodies, examples were drawn from previously identified sites where putative pyroclastic deposits appear to have been sourced from candidate vents within the crater structure, and where those vents are evident in topographic data. On this basis, and choosing examples only where the presence of a pyroclastic deposit is relatively uncontroversial, 15 lunar examples were drawn from 41 possible sites (Wolfe and El-Baz, 1976; Head and Wilson, 1979; Coombs and Hawke, 1992; Gaddis et al., 2003; Gustafson et al., 2012). A sample of 16 sites was drawn from 71 identified sites on Mercury (Kerber et al., 2011; Thomas et al., 2014b). These selection criteria, choosing examples that are least-controversial and most amenable to analysis on each body, may mean that the samples do not reveal the full range of variation in pyroclastic activity within complex craters on either body.

2.2. Pyroclastic deposits

Identification of putative pyroclastic deposits on both Mercury and the Moon relies primarily, at present, on observation of a diffuse-margined spectral anomaly in orbital images. Deposits believed to be pyroclastic on Mercury have higher reflectance and a steeper ("redder") slope of spectral reflectance versus wavelength than the planetary average. To identify them, we constructed composites combining reflectance data from the 996 nm, 749 nm and 433 nm filters in MESSENGER's 10.5° field-of-view Wide Angle Camera (WAC) in the red, green, and blue channels, respectively, in which they appear as a bright, orange spectral anomaly (Fig. 1a). We constructed composites from all images created prior to October 17th, 2013, having a resolution of 1000 m/pixel or better, and also examined the PDS-hosted 1000 m/pixel global color mosaic (March 2014 release).

Lunar pyroclastic deposits are commonly identified by their low albedo relative to highlands material and a spectral character suggesting varying mixtures of highlands, basaltic and glass components (Gaddis et al., 2003). We identified the extent of putative deposits on the basis of a low-albedo, diffuse-margined anomaly in the 1489 nm apparent reflectance mosaic from the Moon Mineralogy Mapper (M3) on the Chandrayaan-1 spacecraft, and in a color composite combining 1000 nm, 900 nm and 415 nm global mosaic reflectivity data from the Clementine spacecraft in the red, green and blue bands (Fig. 1b).

For both bodies, we digitized the areal extent of the spectral anomaly, taking a conservative approach by excluding the tenuous outer fringe. This was further refined in lunar examples where the extent of the low albedo material is apparent as fine-grained material mantling the underlying terrain in high-resolution narrow-angle camera (NAC) images from the Lunar Reconnaissance Orbiter